Rotating full- and reduced-dimensional quantum chemical models of molecules

Csaba Fábri, Edit Mátyus,[a] and Attila G. Császár[b]
Laboratory of Molecular Spectroscopy, Institute of Chemistry, Eötvös University, P.O. Box 32, H-1518 Budapest 112, Hungary

A flexible protocol, applicable to semirigid as well as floppy polyatomic systems, is developed for the variational solution of the rotational–vibrational Schrödinger equation. The kinetic energy operator is expressed in terms of curvilinear coordinates, describing the internal motion, and rotational coordinates, characterizing the orientation of the frame fixed to the nonrigid body. Although the analytic form of the kinetic energy operator might be very complex, it does not need to be known *a priori* within this scheme as it is constructed automatically and numerically whenever needed. The internal coordinates can be chosen to best represent the system of interest and the body-fixed frame is not restricted to an embedding defined with respect to a single reference geometry. The features of the technique mentioned make it especially well suited to treat large-amplitude nuclear motions. Reduced-dimensional rovibrational models can be defined straightforwardly by introducing constraints on the generalized coordinates. In order to demonstrate the flexibility of the protocol and the associated computer code, the inversion-tunneling of the ammonia ($^{14}NH_3$) molecule is studied using one, two, three, four, and six active vibrational degrees of freedom, within both vibrational and rovibrational variational computations. For example, the one-dimensional inversion-tunneling model of ammonia is considered also for nonzero rotational angular momenta. It turns out to be difficult to significantly improve upon this simple model. Rotational–vibrational energy levels are presented for rotational angular momentum quantum numbers $J = 0, 1, 2, 3$, and 4. © *2011 American Institute of Physics*. [doi:10.1063/1.3533950]

I. INTRODUCTION

Large-amplitude motions (LAMs) of molecular systems sample regions of a potential energy surface (PES) either far away from or around several equilibrium configurations. Some of the LAM cases investigated include ring puckering,[1–7] torsional and internal rotation[8–12] or inversion[13–20] motions, bendings in quasilinear molecules,[21–24] tunneling,[25–29] and the interfragment modes of weakly bound complexes.[30–32] These studies prove the general interest and the related challenges one faces when trying to treat these complex motions of the nuclei quantum mechanically. In all these cases traditional quantum mechanical (QM) treatments suitable for (semi)rigid molecules, such as simple vibrational perturbation theory based on the Eckart–Watson (EW) Hamiltonians[33–35] and carried out to second order (VPT2)[36–38] and beyond[39–41] or variational treatments utilizing the exact EW Hamiltonians, are not particularly useful. Extensions offered to the variational EW Hamiltonian treatment (like the reaction path Hamiltonian[42] extension of the widely utilized protocol and code Multimode[43–45]) usually allow the treatment of LAM only along a single coordinate.

Time-independent variational techniques employed in computational molecular spectroscopy, a field of nuclear motion theory, have traditionally been built upon the use of rectilinear normal coordinates, the Eckart embedding, and the resulting Hamiltonians. Nevertheless, for large-amplitude motions one must use curvilinear internal coordinates as only they provide a suitable and efficient physical description and allow to move away from the Eckart frame and not to connect the Hamiltonian to a single reference configuration. Furthermore, since in many cases there is only a small number of (but more than one) internal coordinates that dominate the large-amplitude motions even in relatively complex and large molecules, development of reduced-dimensional (variational) nuclear motion treatments is highly desirable (see, e.g., Refs. 46–49). Recently, two of the authors of this article developed,[50] based also on earlier work,[51–55] an efficient and black-box-type *vibration-only* protocol relying on the use of a Hamiltonian expressed in arbitrary internal coordinates and body-fixed frames. The protocol and the code were termed as GENIUSH, in reference to its main characteristics: General code with Numerical, Internal-coordinate, User-Specified Hamiltonians. The most characteristic advantages of the GENIUSH protocol are that: (a) it is completely general in the sense that a single code could be written to treat *all* molecular systems of feasible size, irrespective of the fact whether their PESs contain a single minimum or easily accessible multiple minima and what the choices of internal coordinates and coordinate system embeddings are; (b) the complex form of the exact kinetic energy operator in internal coordinates, see, e.g., Ref. 56, does not need to be known; and (c) it allows the use of arbitrary reduced-dimensional nuclear motion treatments

---

[a] Current address: Laboratory of Physical Chemistry, ETH Zürich, Wolfgang-Pauli-Str. 10, CH-8093 Zürich, Switzerland.
[b] Author to whom correspondence should be addressed. Electronic mail: csaszar@chem.elte.hu.

within the same code. All these features of the time-independent variational nuclear-motion GENIUSH protocol become especially important when the aim is to treat large-amplitude motions of larger molecular systems. Thus, after finishing the vibration-only part of the GENIUSH code[50] our attention was turned to its extension so that the protocol and the code can handle rotations in full and reduced dimensions, as well.

As to experiments, it is straightforward to learn about large-amplitude motions of molecules by deciphering, with appropriate theoretical tools, their spectral, time-independent consequences. This is because experimentalists have learned a lot about how to improve the resolution when measuring molecular spectra and under high resolution the spectra provide important signatures related to these motions.[57,58] In the case of ammonia (NH$_3$), for example, vibrational motion results in measurable "splittings" which can be turned around to come up with a special potential, connecting two equivalent minima via a small barrier, and an explanation of the spectrum resting on the "umbrella motion." This is a happy state of affairs as now interpretation of experimental molecular spectra of molecules exhibiting large-amplitude nuclear motions can be based on accurate and efficient time-independent quantum mechanical approaches.

Clearly, it is often not sufficient to model high-resolution molecular spectra even through variational quantum chemical computations with zero rotational angular momentum. High-resolution spectra often yield detailed rotational–vibrational information, and thus accurate first-principles computation of rotational–vibrational eigenpairs becomes especially important. Nevertheless, a considerable number of QM nuclear motion protocols developed deal exclusively with the purely vibrational ($J = 0$, where J is the rotational quantum number) problem and only a few have been extended to the simultaneous treatment of excited vibrations and rotations. The variational *rotational–vibrational* QM approaches developed are based either on (a) tailor-made Hamiltonians with explicitly given kinetic energy operators expanded in curvilinear internal coordinates;[59–67] (b) the Eckart–Watson Hamiltonian and rectilinear coordinates;[43,44] or (c) arbitrary vibrational coordinates and numerical construction of the kinetic energy operator.[55,68,69] While the first approach is always limited to special cases as far as the number and connectivity of the atoms are considered, the latter two types of approaches are suitable for arbitrary molecules, though only the third one is fully appropriate when LAMs are considered.

It is usually argued that the rotational problem is less difficult to treat than the vibrational problem. Indeed, the basics of the different variational treatments of rotations is more or less the same, employing such well-established tools as the Euler angles, the rotation matrices forming a complete and finite representation, and the Wang symmetrization.[70,71] Nevertheless, it's still valid to ask whether extension of a GENIUSH-type variational vibrations-only protocol to include rotations would indeed be straightforward or substantial additional difficulties arose in the theory or during programming. One also wonders whether reduced-dimensional models can yield rotational–vibrational eigenvalues compa-

rable in accuracy with the full-dimensional results. Furthermore, given the ease with which one can develop and treat reduced-dimensional models of varying sophistication using GENIUSH, is a reduced-dimensional model treating several additional degrees of freedom indeed considerably more accurate than simple, preferentially 1D models ubiquitously employed in the past? Alternatively, if the reduced-dimensional model is adequate to describe vibrations, would it be similarly adequate to describe rotations and coupling of the two motions? These questions are answered in this paper by reporting the rotational extension of the variational GENIUSH protocol and code and addressing the accuracy issues on the model system of the ammonia molecule (^{14}NH$_3$).

II. THEORY

A. Formulation of the classical Hamiltonian in generalized coordinates

The nonrelativistic Lagrangian of an isolated N-particle system with masses m_i, $i = 1, ..., N$, can be written as

$$L = \frac{1}{2} \sum_{k=1}^{D+6} \sum_{l=1}^{D+6} g_{kl} \dot{q}_k \dot{q}_l - V, \tag{1}$$

where $D < 3N - 6$ for reduced-dimensional models ($D = 3N - 6$ for the full problem), V is the potential energy depending on the coordinates q_k, and

$$g_{kl} = \sum_{i=1}^{N} m_i \frac{\partial \mathbf{X}_i^{\mathrm{T}}}{\partial q_k} \frac{\partial \mathbf{X}_i}{\partial q_l} = \sum_{i=1}^{N} m_i \mathbf{t}_{ik}^{\mathrm{T}} \mathbf{t}_{il}, \quad k, l = 1, \ldots, D+6. \tag{2}$$

In Eq. (2), $\mathbf{X}_i$ is the position vector of the ith atom in the *space-fixed* reference frame (X, Y, Z), and $\mathbf{t}_{ik}$ is the $\mathbf{t}$ vector[72] of the q_k generalized coordinate on the ith atom. After introducing the $p_k = (\partial L / \partial \dot{q}_k)$ ($k = 1, \ldots, D+6$) generalized momenta conjugate to q_k, the classical Hamiltonian takes the following simple form:

$$H = \frac{1}{2} \sum_{k=1}^{D+6} \sum_{l=1}^{D+6} G_{kl} p_k p_l + V, \tag{3}$$

where

$$G_{kl} = \left(\mathbf{g}^{-1} \right)_{kl}, \tag{4}$$

if $\mathbf{g} \in \mathbb{R}^{(D+6) \times (D+6)}$ is not singular.

To construct the $\mathbf{g}$ and $\mathbf{G}$ matrices, let us describe the configuration of the system by the $q_k = q_k$ active ($k = 1, \ldots, D$) and constrained ($k = D + 1, \ldots, 3N - 6$) internal coordinates, the three rotational $q_{D+1} = \alpha_1$, $q_{D+2} = \alpha_2$, $q_{D+3} = \alpha_3$, and the three center-of-mass ($q_{D+4} = X_1^{\mathrm{COM}}$, $q_{D+5} = X_2^{\mathrm{COM}}$, $q_{D+6} = X_3^{\mathrm{COM}}$) coordinates. Then,

$$\mathbf{X}_i = \mathbf{X}^{\mathrm{COM}} + \mathbf{C} \mathbf{x}_i, \quad i = 1, \ldots, N, \tag{5}$$

where $\mathbf{C}$ is an orthogonal rotation matrix depending on the three rotational coordinates, and the $\mathbf{x}_i$ *body-fixed* position vectors in the body-fixed frame (x, y, z) are the functions of

the q_k internal coordinates. Derivation of the g_{kl} matrix elements is equivalent, see Eq. (2), to giving the $\mathbf{t}_{ik}$ vectors in terms of the generalized coordinates.

The *translational* $\mathbf{t}_{i,k+D+3}$ ($k = 1, 2, 3$) vectors are simply

$$t_{i,a,k+D+3} = \frac{\partial X_{ia}}{\partial X_k^{\text{COM}}} = \delta_{ak}, \quad a = 1, 2, 3, \tag{6}$$

where a refers to the three components of the vector $\mathbf{t}$.

By making use of Eq. (2), the translational $\mathbf{g}$ matrix elements can be expressed as

$$g_{k+D+3,l+D+3} = M\delta_{kl}, \quad k, l = 1, 2, 3, \tag{7}$$

where M is the total mass of the system; thus, these are constants.

The *rotational–translational* and the *vibrational–translational* coupling matrix elements of $\mathbf{g}$ are all equal to zero. Therefore, the motion of the center of mass can be separated exactly from the rest of the coordinates. This allows the introduction of the

$$H^{\text{rv}} = T^{\text{rv}} + V = \frac{1}{2}\sum_{k=1}^{D+3}\sum_{l=1}^{D+3} G_{kl}\, p_k p_l + V \tag{8}$$

rovibrational Hamiltonian.

The *rotational* $\mathbf{t}_{i,k+D}$ ($k = 1, 2, 3$) vectors take the form

$$t_{i,a,k+D} = \frac{\partial X_{ia}}{\partial \alpha_k} = \sum_{b=1}^{3}\frac{\partial C_{ab}}{\partial \alpha_k} x_{ib}. \tag{9}$$

Thus, the rotational $\mathbf{g}$ matrix elements are equal to

$$g_{k+D,l+D} = \sum_{i=1}^{N} m_i (\mathbf{e}_k \times \mathbf{x}_i)^{\text{T}}(\mathbf{e}_l \times \mathbf{x}_i), \tag{10}$$

where the direction of the unit vector $\mathbf{e}_k$ coincides with the axis of rotation assigned to the angle α_k [see supplementary material[73] for the derivation of Eq. (10)].

The *vibrational* $\mathbf{t}_{ik}$ ($k = 1, \ldots, D$) vectors are

$$t_{iak} = \frac{\partial X_{ia}}{\partial q_k} = \sum_{b=1}^{3} C_{ab}\frac{\partial x_{ib}}{\partial q_k}. \tag{11}$$

Thus, the corresponding vibrational $\mathbf{g}$ matrix elements are given as

$$g_{kl} = \sum_{i=1}^{N} m_i \frac{\partial \mathbf{x}_i^{\text{T}}}{\partial q_k}\frac{\partial \mathbf{x}_i}{\partial q_l}, \tag{12}$$

where $k, l = 1, \ldots, D$ [see supplementary material[73] for the derivation of Eq. (12)]. To determine g_{kl}, choice of the embedding has to be elucidated, which gives the dependence of the $\mathbf{x}_i$ body-fixed nuclear position vectors on the q_k internal coordinates.

According to the previous expressions, the $\mathbf{g}$ matrix elements of the *rotational–vibrational coupling* block have the form

$$g_{k,l+D} = \sum_{i=1}^{N} m_i \frac{\partial \mathbf{x}_i^{\text{T}}}{\partial q_k}(\mathbf{e}_l \times \mathbf{x}_i), \tag{13}$$

where $k = 1, \ldots, D$, $l = 1, 2, 3$, and $\mathbf{g}$ is a symmetric matrix [see the supplementary material[73] for the derivation of Eq. (13)].

The elements of $\mathbf{G}$ can be expressed in two different ways: (a) by inversion of $\mathbf{g}$ and (b) by introduction of the so-called $\mathbf{s}_{ki}$ vectors,[55,72,74] $\mathbf{s}_{ki} = (\partial q_k/\partial \mathbf{X}_i)$, $k = 1, \ldots, D + 6$ and $i = 1, \ldots, N$. In this study only the first approach has been utilized to construct $\mathbf{G}$.[50]

B. Formulation of the quantum mechanical Hamiltonian in generalized coordinates

In this subsection the rovibrational quantum Hamiltonian $\hat{H}^{\text{rv}}$ is introduced in analogy to the rovibrational classical Hamiltonian H^{rv}. Within the Born–Oppenheimer approximation, the potential energy acting on the nuclei, $\hat{V}$, can be obtained by electronic structure computations. Thus, we will focus on constructing the rovibrational kinetic energy operator in the set of q_k ($k = 1, \ldots, D$) vibrational and α_k ($k = 1, 2, 3$) rotational coordinates. According to differential geometry,[75–77] $\hat{T}^{\text{rv}}$ becomes

$$\hat{T}^{\text{rv}} = \frac{1}{2}\sum_{k=1}^{D+3}\sum_{l=1}^{D+3} \tilde{g}^{-1/4}\hat{p}_k^{\dagger} G_{kl}\tilde{g}^{1/2}\hat{p}_l\tilde{g}^{-1/4}, \tag{14}$$

where $\tilde{g} = \det(\mathbf{g})$, $\mathbf{g}$ is either the full or the rotational–vibrational metric tensor, $\hat{p}_k$ are the quasi-momenta,[78] and the volume element is $dV = d\alpha_1 d\alpha_2 d\alpha_3 dq_1 dq_2 \ldots dq_D$. In units of $\hbar$, for the vibrational coordinates $\hat{p}_k = -i(\partial/\partial q_k)$, $k = 1, \ldots, D$, while for the rotational coordinates $\hat{p}_{k+D} = -i(\partial/\partial\alpha_k)$, $k = 1, 2, 3$, where $i^2 = -1$.

Next, let us utilize that infinitesimal rotations are generated[71] by the projection of the total angular momentum vector $\hat{\mathbf{J}}$ onto the rotational axis:

$$\mathbf{n}\hat{\mathbf{J}} = -i\frac{\partial}{\partial\phi}, \tag{15}$$

where $\mathbf{n}$ has unit length, its direction gives the rotational axis, and ϕ is an angle associated with the rotation around this axis.

After specifying three unique rotational axes, three successive rotations can be performed in order to define the transformation between the space-fixed and body-fixed frames. As the α_k rotational coordinate describes a rotation around the kth of these three rotational axes, it is obvious that

$$\hat{p}_{k+D} = -i\frac{\partial}{\partial\alpha_k} = \hat{J}_k, \tag{16}$$

where $\hat{J}_k$ is the component of the total angular momentum vector along the kth rotational axis. In this study the three rotational axes have been chosen to coincide with the three axes of the body-fixed frame. Therefore, the $\hat{J}_k$ operators correspond to the angular momentum components and the α_k rotational angles define three successive rotations around the three orthogonal axes of the body-fixed system. This study employs these infinitesimal rotational coordinates[79,80] instead of the widely used Eulerian angles. This choice has two significant advantages: (a) one can directly insert the body-fixed components of the total angular momentum into the rovibrational Hamiltonian by utilizing Eq. (16), which greatly reduces the effort to construct $\hat{T}^{\text{rv}}$; and (b) the

rotational and rotational–vibrational blocks of **g** (and thus of **G**) can be computed trivially, as according to Eqs. (10) and (13), one needs to evaluate the $\mathbf{e}_k \times \mathbf{x}_i$ cross products of the unit vectors pointing along the body-fixed axes and the body-fixed atomic position vectors.

C. Variational solution of the rotational–vibrational problem

In order to compute rovibrational states variationally the matrix representation of the $\hat{H}^{\mathrm{rv}}$ Hamiltonian is considered. It is advantageous to split $\hat{T}^{\mathrm{rv}}$ into three terms:

$$\hat{H}^{\mathrm{rv}} = \hat{T}^{\mathrm{rv}} + \hat{V} = \hat{T}^{\mathrm{vib}} + \hat{T}^{\mathrm{rot}} + \hat{T}^{\mathrm{rotvib}} + \hat{V}, \qquad (17)$$

where

$$\hat{T}^{\mathrm{vib}} = \frac{1}{2} \sum_{k=1}^{D} \sum_{l=1}^{D} \tilde{g}^{-1/4} \hat{p}_k^{\dagger} G_{kl} \tilde{g}^{1/2} \hat{p}_l \tilde{g}^{-1/4}, \qquad (18)$$

$$\hat{T}^{\mathrm{rot}} = \frac{1}{2} \sum_{k=1}^{3} G_{k+D,k+D} \hat{J}_k^2 + \frac{1}{2} \sum_{k=1}^{3} \sum_{l>k}^{3} G_{k+D,l+D} [\hat{J}_k, \hat{J}_l]_+, \qquad (19)$$

and

$$\hat{T}^{\mathrm{rotvib}} = \frac{1}{2} \sum_{l=1}^{3} \sum_{k=1}^{D} \left(\tilde{g}^{-1/4} \hat{p}_k^{\dagger} G_{k,l+D} \tilde{g}^{1/4} \right.$$
$$\left. + \tilde{g}^{1/4} G_{k,l+D} \hat{p}_k \tilde{g}^{-1/4} \right) \hat{J}_l, \qquad (20)$$

where $\hat{T}^{\mathrm{vib}}$ is the vibrational and $\hat{T}^{\mathrm{rot}}$ is the rotational kinetic energy and $\hat{T}^{\mathrm{rotvib}}$ gives the coupling between vibrations and rotations. In Eq. (19), $\hat{J}_k$ is the kth body-fixed component of $\hat{\mathbf{J}}$ and $[\hat{J}_k, \hat{J}_l]_+$ refers to the anticommutator of the operators $\hat{J}_k$ and $\hat{J}_l$.

As the $\hat{J}_k$ angular momentum components correspond to the body-fixed frame, they satisfy the anomalous commutation relations[71]

$$[\hat{J}_k, \hat{J}_l] = -i\epsilon_{klm} \hat{J}_m, \qquad (21)$$

where $k, l, m = 1(x), 2(y), 3(z)$, ϵ_{klm} is the Levi–Cività permutation symbol, and the Einstein summation convention is implied. For a given rotational angular momentum quantum number J (the molecular system is isolated and no external fields are present), the set of orthonormal $|JKM\rangle$ symmetric rigid rotor eigenfunctions serves as a suitable basis to set up the matrix representation of $\hat{H}^{\mathrm{rv}}$. According to Eqs. (19) and (20), the matrix representation of $\hat{J}_k$, $\hat{J}_k^2$, and $[\hat{J}_k, \hat{J}_l]_+$ is required to solve the rovibrational problem. The complete set of nonzero $\hat{J}_k$ matrix elements[71] is given by

$$\langle JKM|\hat{J}_x|J(K \pm 1)M\rangle = \frac{1}{2}\sqrt{J(J+1) - K(K \pm 1)},$$

$$\langle JKM|\hat{J}_y|J(K \pm 1)M\rangle = \mp\frac{i}{2}\sqrt{J(J+1) - K(K \pm 1)}, \qquad (22)$$

$$\langle JKM|\hat{J}_z|JKM\rangle = K,$$

where $K = -J, \ldots, J$ corresponds to the body-fixed z, while $M = -J, \ldots, J$ to the space-fixed Z components of the angular momentum. The $\hat{J}_k^2$ and $[\hat{J}_k, \hat{J}_l]_+$ matrices can be constructed by simple matrix multiplication, by inserting the resolution of identity between $\hat{J}_k$ and $\hat{J}_l$, and thus

$$\langle JKM|\hat{J}_k\hat{J}_l|JK'M\rangle$$

$$= \sum_{J'} \sum_{K''=-J'}^{J'} \langle JKM|\hat{J}_k|J'K''M\rangle\langle J'K''M|\hat{J}_l|JK'M\rangle$$

$$= \sum_{K''=-J}^{J} \langle JKM|\hat{J}_k|JK''M\rangle\langle JK''M|\hat{J}_l|JK'M\rangle. \qquad (23)$$

It is important to emphasize that Eq. (23) does not utilize any approximations as

$$\langle JKM|\hat{J}_k|J'K''M\rangle = \delta_{JJ'}\langle JKM|\hat{J}_k|JK''M\rangle. \qquad (24)$$

As a next step, a more sophisticated rotational basis of $2J + 1$ orthonormal Wang functions[71] is introduced by

$$\frac{1}{\sqrt{2}}\left(|JKM\rangle + |J-KM\rangle\right), \quad \text{where } K \text{ is even,}$$

$$\frac{1}{\sqrt{2}}\left(|JKM\rangle - |J-KM\rangle\right), \quad \text{where } K \text{ is odd,}$$

$$\frac{i}{\sqrt{2}}\left(|JKM\rangle - |J-KM\rangle\right), \quad \text{where } K \text{ is even,} \qquad (25)$$

$$\frac{i}{\sqrt{2}}\left(|JKM\rangle + |J-KM\rangle\right), \quad \text{where } K \text{ is odd.}$$

This basis has two advantages over the simple $|JKM\rangle$ functions: (a) after some trivial algebra and careful choice of the vibrational basis, it is revealed that the matrix representation of $\hat{H}^{\mathrm{rv}}$, $\mathbf{H}^{\mathrm{rv}}$, lacks complex matrix elements; and (b) as shown in the previous four equations, one can separate the Wang functions into four (only three for $J = 1$) sets according to the irreducible representations of the D_2 rotational group, which helps exploiting molecular symmetry during the rovibrational computations.

Construction of $\mathbf{H}^{\mathrm{rv}}$ requires the introduction of a rovibrational basis, chosen here as a direct product of the set of vibrational basis functions and $2J + 1$ Wang functions (details concerning the vibrational basis and the necessary matrix elements can be found in Ref. 50). Using Eqs. (17)–(20), $\mathbf{H}^{\mathrm{rv}}$ takes the form

$$\mathbf{H}^{\mathrm{rv}} = \mathbf{T}^{\mathrm{rv}} + \mathbf{V} = \mathbf{T}^{\mathrm{vib}} + \mathbf{T}^{\mathrm{rot}} + \mathbf{T}^{\mathrm{rotvib}} + \mathbf{V}, \qquad (26)$$

where

$$\mathbf{T}^{\mathrm{vib}} = \frac{1}{2}\mathbf{I}_{2J+1} \otimes \sum_{k=1}^{D} \sum_{l=1}^{D} \tilde{\mathbf{g}}^{-1/4} \mathbf{p}_k^{\dagger} \mathbf{G}_{kl} \tilde{\mathbf{g}}^{1/2} \mathbf{p}_l \tilde{\mathbf{g}}^{-1/4}, \qquad (27)$$

$$\mathbf{T}^{\mathrm{rot}} = \frac{1}{2} \sum_{k=1}^{3} \mathbf{J}_k^2 \otimes \mathbf{G}_{k+D,k+D}$$

$$+ \frac{1}{2} \sum_{k=1}^{3} \sum_{l>k}^{3} [\mathbf{J}_k, \mathbf{J}_l]_+ \otimes \mathbf{G}_{k+D,l+D}, \qquad (28)$$

TABLE I. Z-matrix representation of the internal coordinates of NH$_3$.

N						
X	N	1.0				
H$_1$	N	r_1	X	θ		
H$_2$	N	r_2	X	θ	H$_1$	β_1
H$_3$	N	r_3	X	θ	H$_1$	$-\beta_2$

and

$$
\mathbf{T}^{\text{rotvib}} = \frac{1}{2} \sum_{l=1}^{3} \mathbf{J}_l \otimes \sum_{k=1}^{D} \left(\tilde{\mathbf{g}}^{-1/4} \mathbf{p}_k^{\dagger} \mathbf{G}_{k,l+D} \, \tilde{\mathbf{g}}^{1/4} \right.
$$
$$
\left. + \, \tilde{\mathbf{g}}^{1/4} \mathbf{G}_{k,l+D} \, \mathbf{p}_k \tilde{\mathbf{g}}^{-1/4} \right), \tag{29}
$$

where $\mathbf{I}_{2J+1}$ is the identity matrix of dimension $2J+1$ and $\otimes$ refers to the direct product operation.

The iterative Lanczos algorithm[81] has been utilized to compute the required eigenvalues and eigenvectors of $\mathbf{H}^{\text{rv}}$ which only needs the effect of $\mathbf{H}^{\text{rv}}$ on an arbitrary vector of the same dimension upon matrix-vector multiplication. As $\mathbf{H}^{\text{rv}}$ has a special and very sparse structure, it is not constructed explicitly during the computation. Instead, the $\mathbf{H}^{\text{rv}}\mathbf{x}$ matrix–vector multiplication is implemented, similarly to Ref. 50, which reduces computation cost and memory requirements.

III. COMPUTATIONAL DETAILS

The PES of ^{14}NH$_3$ employed in this study was taken from Ref. 82. It corresponds to the PES called "refined" in that study. Atomic masses, $m_H = 1.007\,825$ u and $m_N = 14.003\,074$ u, were employed throughout the nuclear motion computations. The set of internal coordinates applied is summarized in Table I. The embedding of the rotational axes was done as follows: (a) the origin of the body-fixed frame is placed on the first atom (N); (b) the x axis is directed toward the second atom (X, a dummy atom); (c) the $x - y$ plane is defined by the first three atoms (N, X, and H$_1$); (d) the z axis is oriented according to the right-hand rule; and (e) the origin is shifted to the center of mass of the nuclei. For reference purposes, full-dimensional variational rovibrational computations employing the complete rovibrational Hamiltonian without constraints on the coordinates were carried out.

Besides the full-dimensional, 6D, model, five reduced-dimensional models, henceforth called 1D, 2D, 3D, 4D$_1$, and 4D$_2$, were also implemented, where the number of dimensions refers to the number of active vibrational coordinates. In all reduced-dimensional models the coordinate θ,

describing the inversion motion, was kept active. Different symmetrized and nonsymmetrized stretching and bending coordinates were added to it in order to investigate their effect on the rovibrational states. The models are shown in Table II, detailing both the active and the constrained coordinates. The constrained coordinates were fixed at the equilibrium values of the PES, $r_1 = r_2 = r_3 = 1.01031$ Å and $\beta_1 = \beta_2 = 120^{\circ}$. Fixing these coordinates is equivalent to the deletion of rows and columns corresponding to the constrained coordinates from the full-dimensional $\mathbf{g}$ matrix. An alternative method had also been implemented for the 4D$_1$ model, whereby values of the constrained β_1 and β_2 coordinates were allowed to relax at each grid point of the active coordinates. For the lower lying vibrational levels computed the "relaxed" and "fixed" results show no significant deviations. This result validates our choice of equilibrium values for the constrained coordinates, at least for the lower lying vibrational levels. Implementation of all these different models is straightforward within the GENIUSH protocol.

Potential-optimized (PO) (Refs. 83–85) Hermite-DVR (where DVR means discrete variable representation) basis functions were utilized for the vibrational degrees of freedom, see Ref. 50 for details. The DVR intervals for the internal coordinates can be summarized as follows: $r_1, r_2, r_3 \in [0.35, 2.5]$ Å, $\beta_1, \beta_2 \in [20, 220]^{\circ}$, and $\theta \in [5, 175]^{\circ}$. In this study the Podolsky form[50] of the kinetic energy operator given in Eqs. (14) and (17)–(20) has been applied without further rearrangement. It requires the evaluation of only the first derivatives of the Cartesian coordinates in the body-fixed frame with respect to the internal coordinates, unlike the "rearranged" form[50] often used in (ro)vibrational computations,[52,54,55] which requires not only the first but also the second and third derivatives. The rovibrational protocol presented in this work for the Podolsky form can be easily adapted to the case of the "rearranged" Hamiltonian.

The customary ordering of the vibrational quantum numbers is employed for labeling the computed $J = 0$ states: 1 = totally symmetric stretch, 2 = inversion mode, 3 = doubly degenerate stretch, and 4 = doubly degenerate bend. The inversion-mode states are labeled, however, not by v_2 but by v_{inv} to account for the doubling of the levels. The molecular symmetry (MS) (Refs. 58 and 86) group $D_{3h}(M)$ is used to provide labels for the symmetries of the rotational–vibrational states of ammonia.

The pure electronic and effective 1D vibrationally averaged barriers to inversion of ^{14}NH$_3$ are computed to be 1777 ± 10 and 2021 ± 20 cm^{-1}, respectively.[87,88] The latter value is in full agreement with a set of effective 1D spectroscopic results in the 2018 ± 10 cm^{-1} interval.[13–16] This

TABLE II. Characteristics of the reduced-dimensional models of NH$_3$ employed in this study.

Model	Active coordinates	Constrained coordinates	N_b for the active DOFs[a]
1D	θ	$r_1, r_2, r_3, \beta_1, \beta_2$	40 (100)
2D	$\theta, \frac{1}{\sqrt{3}}(r_1 + r_2 + r_3)$	$\frac{1}{\sqrt{6}}(2r_1 - r_2 - r_3), \frac{1}{\sqrt{2}}(r_2 - r_3), \beta_1, \beta_2$	25 (80), 15 (80)
3D	θ, β_1, β_2	r_1, r_2, r_3	25 (80), 15 (80), 15 (80)
4D$_1$	θ, r_1, r_2, r_3	β_1, β_2	25 (80), 15 (80), 15 (80), 15 (80)
4D$_2$	$\theta, \frac{1}{\sqrt{3}}(r_1 + r_2 + r_3), \beta_1, \beta_2$	$\frac{1}{\sqrt{6}}(2r_1 - r_2 - r_3), \frac{1}{\sqrt{2}}(r_2 - r_3)$	25 (80), 15 (80), 15 (80), 15 (80)

[a]N_b = number of basis functions. DOF = degree of freedom. The number of primitive DVR vibrational basis functions is given in parentheses.

TABLE III. Relevant full- and reduced-dimensional zero-point vibrational energies (GS = ground state) and vibrational band origins of $^{14}NH_3$ relative to the vibrational ground state energy, all in cm^{-1}. The molecular symmetry group $D_{3h}(M)$ is used to label the rotational–vibrational states of ammonia. The $D_{3h}(M)$ symmetry labels are given in parentheses. The 1D, 2D, and 4D$_1$ models do not exhibit the ν_4^+ and ν_4^- vibrations as the β_1 and β_2 vibrational coordinates are fixed in these cases.

	1D	2D	3D	4D$_1$	4D$_2$	6D	Expt.[a]
0^+ (A_1', GS)	521.43	2256.74	2158.70	5828.91	3911.34	7436.82	...
0^- (A_2'')	1.13	1.28	1.70	0.58	1.74	0.79	0.79
ν_2^+ (A_1')	930.57	900.48	904.48	945.65	881.01	932.41	932.43
ν_2^- (A_2'')	979.80	952.80	970.68	973.89	946.02	968.15	968.12
$2\nu_2^+$(A_1')	1586.97	1537.60	1550.06	1626.11	1511.43	1597.26	1597.47
ν_4^+ (E')	...	...	1659.43	...	1649.71	1625.62	1626.28
ν_4^- (E'')	...	...	1662.12	...	1652.08	1626.73	1627.37
$2\nu_2^-$(A_2'')	1918.86	1868.39	1917.98	1884.43	1867.66	1882.18	1882.18

[a]Experimental results are taken from Ref. 90 and have higher accuracy than indicated here. The VBOs obtained with TROVE,[82,91] using the same PES and following the same order, are 7436.82, 0.80, 932.42, 968.16, 1597.29, 1625.64, 1626.75, and 1882.20 cm^{-1}.

energy is smaller than all but five of the vibrational state energies of $^{14}NH_3$. The vibrational band origins (VBOs) of $^{14}NH_3$ lower than this energy have quantum numbers $v_{inv} = 0, 1, 2$, and 3, and $v_4 = 1$. This investigation focuses only on the rotational–vibrational states characterized by $v_{inv} = 0, 1, 2, 3, 4$, and 5 and $v_4 = 1$, while all other vibrational quantum numbers are kept at zero.

Ideally, each inversion state holds a set of $2J + 1$ "rotational" energy levels which can be characterized as symmetric top levels using the usual quantum numbers J and K.[58] To label the rotational–vibrational states of ammonia further, two routes can be followed. The clearest route is to use the v_{inv} quantum number to distinguish between the inversion doublets and employ the irreducible representations of the $D_{3h}(M)$ MS group. The less preferred alternative is to designate the doublets with superscripted $+$ and $-$ symbols, indicating the lower and higher energy member of the pairs, respectively. Note also that nuclear spin statistics makes some of the computed rovibrational levels missing. Finally, we mention that for the $\{\nu_2^+, \nu_2^-\}$ diad and especially for the $\{2\nu_2^+, \nu_4^+, \nu_4^-\}$ triad, the energy order of the rotational–vibrational eigenstates does not strictly follow the order of the VBOs (the $J = 0$ eigenstates). The rotational–vibrational states were sorted according to the prescription of the rigid-rotor decomposition (RRD) procedure as given in Ref. 89.

IV. RESULTS AND DISCUSSION

A. Full-dimensional results

The full (6D) dimensional VBOs obtained with the PES and the exact kinetic energy operator employed in this study within the GENIUSH protocol have been reported in Ref. 50. A few of these results are reproduced in Table III along with the experimental values taken from Ref. 90. The basis set used here is large enough to converge all the VBOs of interest to better than 0.01 cm^{-1}. Thus, the computed full-dimensional rotational–vibrational energy levels, some of which are reported in Table IV, serve as benchmark numbers.

As clear from Table IV, the present PES,[82] at least for the low J values investigated in this study, provides rotational–vibrational energies in good agreement with the experimental results (not shown). The agreement is not as outstanding as

has been observed for the recent exceedingly high quality *ab initio* and *ab initio*-based PESs of water,[92–94] but the average accuracy of the computed lines is down to the 0.1 cm^{-1} level.

It is also interesting to compare the present benchmark energy values to those obtained using the TROVE algorithm employing truncated kinetic and potential energy operators.[82,91] The appropriate vibrational and rovibrational results are reported in Tables III and IV, respectively. In all cases the TROVE energy values are higher than the GENIUSH ones. However, the differences are very small, on the order of 0.01–0.03 cm^{-1}, both for the pure vibrational and rovibrational states, considerably smaller than the accuracy of the PES employed, on the order of 0.1 cm^{-1} for the states considered. This proves the validity and utility of the approximations introduced in the TROVE algorithm.

Finally, a few words about the rotational wave numbers corresponding to the different rotational axes. The rotational energies at about 20 cm^{-1} for $J = 1$ are considerably larger than the splitting between the 0^+ and 0^- states, about 1 cm^{-1}. Thus, resonance interactions should be limited. One further expects that rotation about the principal symmetry axis increases the inversion splitting and those about the perpendicular axes act in the opposite direction. As shown in Fig. 1, the splittings between the E' and E'' states can both increase and decrease as a function of J and K, though these changes are rather small for the small J values considered. The relative splittings change almost linearly as a function of K. For each J, the relative splitting is positive only for the largest K pair.

B. Convergence of the rovibrational levels

Convergence of the rovibrational levels of NH$_3$ was examined extensively with respect to the size of the vibrational basis. Full-dimensional computations were carried out from $J = 0$ up to $J = 4$. The reported "convergent" results were computed using 25 vibrational basis functions for the inversion and 10 vibrational basis functions for each of the other five degrees of freedom. For the approximate rovibrational levels a considerably smaller vibrational basis, containing 14 functions for the inversion and 5 for each of the others, was utilized. The basis functions mentioned refer to PO DVR

TABLE IV. Selected computed full-dimensional rotational–vibrational energy levels of $^{14}NH_3$ for $J = 1-4$, in cm^{-1}, referenced to the zero-point vibrational energy of the system (all vibrational modes other than the umbrella motion remain in their ground state). See text for the meaning of the labels $\{v_{inv}\, JK\}$ of the rotational–vibrational states. Symmetry labels correspond to the $D_{3h}(M)$ molecular symmetry group.

J	K	v_{inv}	Symm. label	GENIUSH	TROVE
1	0	0	A_2'	19.907	19.907
1	1	0	E''	16.188	16.188
1	1	1	E'	16.979	16.981
1	0	2	A_2'	952.558	952.570
1	1	2	E''	948.578	948.589
1	1	3	E'	984.209	984.219
2	1	0	E''	55.988	55.988
2	2	0	E'	44.838	44.838
2	0	1	A_2''	60.465	60.467
2	1	1	E'	56.759	56.761
2	2	1	E''	45.630	45.632
2	1	2	E''	988.860	988.872
2	2	2	E'	976.928	976.940
2	0	3	A_2''	1027.507	1027.517
2	1	3	E'	1023.781	1023.792
2	2	3	E''	1012.596	1012.606
3	0	0	A_2'	119.341	119.342
3	1	0	E''	115.637	115.638
3	2	0	E'	104.516	104.516
3	3	0	A_2''	85.943	85.944
3	1	1	E'	116.380	116.382
3	2	1	E''	105.278	105.280
3	3	1	A_2''	86.740	86.742
3	0	2	A_2'	1053.171	1053.183
3	1	2	E''	1049.216	1049.228
3	2	2	E'	1037.327	1037.340
3	3	2	A_2''	1017.453	1017.465
3	1	3	E'	1083.098	1083.109
3	2	3	E''	1071.935	1071.946
3	3	3	A_2'	1053.302	1053.313
4	1	0	E''	195.076	195.077
4	2	0	E'	183.991	183.992
4	3	0	E''	165.482	165.482
4	4	0	E'	139.492	139.492
4	0	1	A_2'	199.466	199.469
4	1	1	E'	195.781	195.784
4	2	1	E''	184.716	184.719
4	3	1	A_2'	166.239	166.242
4	4	1	E''	140.298	140.300
4	1	2	E''	1129.566	1129.579
4	2	2	E'	1117.734	1117.747
4	3	2	A_2''	1097.956	1097.969
4	4	2	E'	1070.140	1070.152
4	0	3	A_2''	1165.817	1165.829
4	1	3	E'	1162.108	1162.121
4	2	3	E''	1150.975	1150.988
4	3	3	A_2'	1132.390	1132.403
4	4	3	E''	1106.313	1106.324

functions for all degrees of freedom, each of them were generated by employing 80 primitive DVR functions (see Table II for a summary about basis functions for the reduced-dimensional models).

A pictorial representation of the deviations between the convergent and approximate rovibrational levels is given in Fig. S1 of supplementary material,[73] where the minimum unsigned, maximum unsigned, and mean values of these deviations are plotted for six vibrational states.

As usual, deviations between the convergent and the approximate rovibrational levels increase with vibrational excitation. For the vibrational ground state the small vibrational basis is able to reproduce the exact rovibrational levels very well, while the biggest deviations are present for the fifth VBO. These findings suggest that: (a) the incompleteness of the vibrational basis plays an important role in the error of the rovibrational levels (unless they are referenced to the actual VBO); and (b) even small vibrational basis sets are able to supply rovibrational levels of appropriate precision for some of the vibrational band origins.

C. Reduced-dimensional results

During the present test study of $^{14}NH_3$, five reduced-dimensional models (see Table II) have been tested, ranging from 1D to 4D. Table II summarizes some details concerning the number of applied vibrational basis sets for the vibrational models. Table III gives the computed full- and reduced-dimensional vibrational band origins of interest for this study. All of the computed rovibrational levels were referenced to the appropriate VBOs and the differences of these full- and reduced-dimensional levels were then computed. The maximum unsigned, minimum unsigned, and mean absolute deviations (MADs) are summarized in Table V for $J = 1$ and 4, respectively.

The zero-point vibrational energy (ZPVE) for the 1D model is 521.4 cm^{-1} (Table IV). The considerable increase in the effective 1D barrier height mentioned before is due to the significant tightening of bonding at the transition state, as reflected in the PES. In the 1D model, similarly to the full 6D model, there are four vibrational states below the barrier, while the fifth state ($v_{inv} = 4$) is already slightly beyond it.

Though there is a considerable shift (see the MAD values of Table V) of the rovibrational energy levels due to the incompleteness of the vibrational model for the ground state, deviations from the MADs are considerably smaller, up to a factor of 6. Thus, the computed reduced-dimensional rovibrational energies have considerable predictive power.

The summary of the computed deviations of the reduced-dimensional rotational–vibrational results from the full rovibrational results (Table V) shows clearly the considerable approximations characterizing the 1D vibrational model. Interestingly, the 2D model, employing the two fully symmetric modes of ammonia, does not improve substantially the 1D results, except for the 0^+ and 0^- states. For example, the difference between the $2\nu_2^+(A_1')$ and $2\nu_2^-(A_1'')$ VBOs is 285 cm^{-1} experimentally, while the $\{1D, 2D\}$ splittings are $\{332, 331\}$ cm^{-1}, a gross overestimation in both cases. In fact, none of the reduced-dimensional models are successful in predicting this splitting.

By far the best model for describing the umbrella motion of ammonia is the $4D_1$ model. This is a somewhat
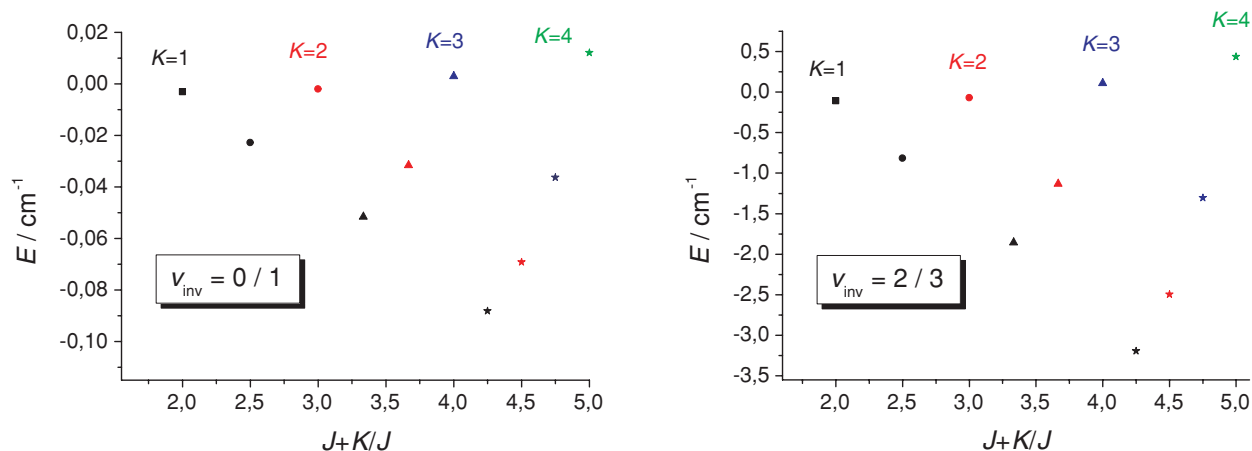
FIG. 1. Relative splittings between rovibrational states of $^{14}NH_3$ sharing the same K value for a given J for the $v_{inv} = 0/1$ ($v_2 = 0$) and $v_{inv} = 2/3$ ($v_2 = 1$) pairs, referenced to the corresponding $J = 0$ values. Relative splittings for different J values are denoted according to the following pattern: rectangle: $J = 1$, circle: $J = 2$, triangle: $J = 3$, and star: $J = 4$.

nonintuitive result and perhaps stems from a considerable coupling between the umbrella mode and the overtones of the nonsymmetric stretching modes. Nevertheless, even this best reduced-dimensional model produces errors an order of magnitude larger than the intrinsic accuracy of the PES. Even in the most favorable cases the improvement in the maximum unsigned error is only about a factor of 2. Thus, it is surprisingly hard to improve upon the simplest 1D model by the

inclusion of further degrees of freedom in the active set of coordinates. This is a serious warning when treating larger, more complex systems and what can be expected from models including several degrees of freedom in the active set designed to improve upon the physically simplest model. However, in the many cases when the smallest reasonable treatment of the molecular system does require the active treatment of several coordinates, the present procedure provides

TABLE V. Maximum unsigned, minimum unsigned, and MAD deviations between the computed full- and reduced-dimensional results, in cm^{-1}, for the $J = 1$ and $J = 4$ states of $^{14}NH_3$. Both the full- and the reduced-dimensional rovibrational levels are referenced to the appropriate vibrational band origins given in Table III.

Label		$J = 1$					$J = 4$				
		1D	2D	3D	$4D_1$	$4D_2$	1D	2D	3D	$4D_1$	$4D_2$
0^+	maximum	0.243	0.129	1.360	0.343	0.461	2.697	1.376	6.570	3.282	4.606
	minimum	0.208	0.121	1.087	0.195	0.271	1.909	1.351	2.360	1.050	1.571
	MAD	0.219	0.127	1.178	0.244	0.334	2.357	1.362	4.815	2.359	3.344
0^-	maximum	0.247	0.130	1.448	0.338	3.444	2.731	1.377	6.527	3.239	4.516
	minimum	0.211	0.121	1.180	0.193	0.268	1.939	1.357	2.401	1.049	1.587
	MAD	0.223	0.127	1.270	0.242	1.327	2.390	1.365	4.806	2.334	3.297
v_2^+	maximum	0.440	0.491	2.542	0.125	0.698	4.742	5.114	9.500	4.755	7.790
	minimum	0.254	0.290	2.163	0.075	0.351	1.450	1.716	1.243	0.438	1.441
	MAD	0.316	0.357	2.416	0.092	0.467	3.351	3.685	5.263	1.645	4.930
v_2^-	maximum	0.596	0.530	0.349	0.024	0.529	6.181	5.417	6.557	3.650	5.308
	minimum	0.372	0.332	0.074	0.015	0.309	2.420	2.155	0.499	0.148	0.611
	MAD	0.447	0.398	0.166	0.018	0.382	4.607	4.053	4.155	0.860	3.576
v_4^+	maximum	...	...	1.063	...	0.932	...	...	8.502	...	5.589
	minimum	...	...	0.014	...	0.256	...	...	1.386	...	0.065
	MAD	...	...	0.622	...	0.552	...	...	6.207	...	3.829
v_4^-	maximum	...	...	1.079	...	0.942	...	...	8.431	...	5.483
	minimum	...	...	0.030	...	0.273	...	...	1.384	...	0.097
	MAD	...	...	0.587	...	0.508	...	...	5.684	...	3.219
$2v_2^+$	maximum	0.500	0.617	3.462	0.275	0.470	4.950	6.061	3.781	2.573	4.564
	minimum	0.293	0.396	3.332	0.086	0.319	1.795	2.716	1.919	0.199	2.358
	MAD	0.362	0.470	3.419	0.149	0.369	3.717	4.749	3.082	1.598	3.723
$2v_2^-$	maximum	1.012	0.894	1.713	0.424	0.478	10.209	8.957	6.359	4.231	4.799
	minimum	0.607	0.529	1.505	0.171	0.313	3.683	3.117	3.075	0.197	2.148
	MAD	0.742	0.651	1.574	0.255	0.368	7.495	6.530	4.990	2.558	3.695

a straightforward way for the interpretation of the measured rotational–vibrational spectra.

V. SUMMARY

By extending a previous vibration-only study,[50] laying down the foundation of the GENIUSH protocol, where GENIUSH stands for General algorithm with Numerical, Internal-coordinate, User-Specified Hamiltonians, a fully general quantum mechanical algorithm is presented here which treats the rotational and vibrational degrees of freedom of free molecules simultaneously. The rotational–vibrational GENIUSH protocol can employ a set of arbitrary curvilinear vibrational coordinates to describe the internal motion of the molecule. Note that the protocol was not developed based on the ubiquitous Euler angles to describe the overall rotation of the molecule but on infinitesimal rotations. The thus completed nuclear motion GENIUSH algorithm allows computation of full-dimensional rotational–vibrational eigenstates with an exact kinetic energy operator whose form does not need to be known in advance. Due to its design, the GENIUSH algorithm is perfectly suitable to treat molecules exhibiting an arbitrary number of large-amplitude motions connecting an arbitrary number of minima on the potential energy surface of the molecule. A potentially even more significant advantage of this protocol over other existing schemes is that it is developed to allow the design of different reduced-dimensional nuclear motion computations and execute them within exactly the same code. Finally, it is noted that in several instances the overall rotation of the molecule cannot be separated from the large-amplitude motions due to the similarity in their time scales. The GENIUSH protocol can be employed in these cases straightforwardly. In quantum control theory of molecular systems,[95] J seizes to be a good quantum number due to the presence of an external field, and algorithms treating vibrations and rotations on an equal footing should be employed, like the general GENIUSH protocol.

The capabilities of the rovibrational GENIUSH algorithm were tested on the ammonia ($^{14}NH_3$) molecule, exhibiting one large-amplitude motion usually called "umbrella motion." Rovibrational energy results from five reduced-dimensional models were compared to the full 9D treatment of coupled internal and rotational motions of ammonia. The rovibrational energy levels obtained from even just a 1D vibrational treatment agree nicely with those from the full treatment. This suggests that reduced-dimensional computations can yield reasonably accurate rotational–vibrational eigenenergies (and eigenfunctions) if the reduced-dimensional vibrational model is reasonably accurate. The deviations between the 1D and full-D energies increase considerably for the excited vibrations. This increase is mostly due to the discrepancies in the vibrational band origins, but some of it remains when the rovibrational energies are referenced to the appropriate VBOs. From the different computations employing 1D, 2D, 3D, 4D, and 6D vibrational models, always including the umbrella motion of ammonia, it is clear that the simplest 1D model is successful in reproducing the splitting of the first few pairs of VBOs and that of the rotational levels they hold with respect to experiments and it is rather hard to substan-

tially improve upon it. Nevertheless, in the many known cases when even the smallest reasonable treatment of the molecular system exhibiting large-amplitude motions requires the active treatment of several degrees of freedom, the GENIUSH protocol, or any similar procedure, provides a straightforward way for the interpretation of the measured rotational–vibrational spectra via reduced-dimensional nuclear motion computations.

ACKNOWLEDGMENTS

[1] J. Laane, in *Vibrational Spectra and Structure*, edited by J. R. Durig (M. Dekker, New York, 1972), Vol. I, pp. 25–50.

[2] W. D. Allen, A. G. Császár, and D. A. Horner, J. Am. Chem. Soc. **114**, 6834 (1992).

[3] V. Szalay, G. Bánhegyi, and G. Fogarasi, J. Mol. Spectrosc. **126**, 1 (1987).

[4] H. L. Strauss, Annu. Rev. Phys. Chem. **34**, 301 (1983).

[5] A. C. Legon, Chem. Rev. **80**, 231 (1980).

[6] E. Czinki and A. G. Császár, Chem.-Eur. J. **9**, 1008 (2003).

[7] L. A. Carreira, R. C. Lord, and T. B. Malloy, Jr., Top. Curr. Chem. **82**, 1 (1979).

[8] J. B. Howard, J. Chem. Phys. **5**, 451 (1937).

[9] M. Ribeaud, A. Bauder, and H. H. Günthard, Mol. Phys. **23**, 235 (1972).

[10] J.-M. Flaud, C. Camy-Peyret, J. W. C. Johns, and B. Carli, J. Chem. Phys. **91**, 1504 (1989).

[11] J. Plíva, A. S. Pine, and S. Civis, J. Mol. Spectrosc. **180**, 15 (1996).

[12] A. G. Császár, V. Szalay, and M. L. Senent, J. Chem. Phys. **120**, 1203 (2004).

[13] J. D. Swalen and J. A. Ibers, J. Chem. Phys. **36**, 1914 (1962).

[14] D. Papoušek and V. Špirko, Top. Curr. Chem. **68**, 59 (1976).

[15] V. Špirko, J. Mol. Spectrosc. **101**, 30 (1983).

[16] V. Špirko and W. P. Kraemer, J. Mol. Spectrosc. **133**, 331 (1989).

[17] E. Kauppi and L. Halonen, J. Chem. Phys. **103**, 6861 (1995).

[18] C. Puzzarini, Theor. Chem. Acc. **121**, 1 (2008).

[19] T. Rajamäki, M. Kállay, J. Noga, P. Valiron, and L. Halonen, Mol. Phys. **102**, 2297 (2004).

[20] R. Marquardt, K. Sagui, W. Klopper, and M. Quack, J. Phys. Chem. B **109**, 8439 (2005).

[21] R. N. Dixon, Trans. Faraday Soc. **60**, 1363 (1964).

[22] P. R. Bunker and D. J. Howe, J. Mol. Spectrosc. **83**, 288 (1980).

[23] P. Jensen, Comput. Phys. Commun. **1**, 1 (1983).

[24] M. A. King, H. W. Kroto, and B. M. Landsberg, J. Mol. Spectrosc. **113**, 1 (1985).

[25] R. P. Bell, *The Tunnel Effect in Chemistry* (Chapman and Hall, New York, 1980).

[26] F. L. Bettens, R. P. A. Bettens, R. D. Brown, and P. D. Godfrey, J. Am. Chem. Soc. **122**, 5856 (2000).

[27] G. C. Schatz, Chem. Rev. **87**, 81 (1987).

[28] K. Tanaka, M. Toshimitsu, K. Harada, and T. Tanaka, J. Chem. Phys. **120**, 3604 (2004).

[29] P. R. Schreiner, H. P. Reisenauer, F. C. Pickard, A. C. Simmonett, W. D. Allen, E. Mátyus, and A. G. Császár, Nature (London) **453**, 906 (2008).

[30] D. J. Wales, in *Computational Molecular Spectroscopy*, edited by P. Jensen and P. R. Bunker (Wiley, Chichester, 2000), pp. 431–456.

[31] W. Klopper, M. Quack, and M. A. Suhm, J. Chem. Phys. **108**, 10096 (1998).

[32] G. W. M. Vissers, G. C. Groenenboom, and A. van der Avoird, J. Chem. Phys. **119**, 277 (2003).

[33] C. Eckart, Phys. Rev. **47**, 552 (1935).

[34] J. K. G. Watson, Mol. Phys. **15**, 479 (1968).

[35] J. K. G. Watson, Mol. Phys. **19**, 465 (1970).

[36] H. H. Nielsen, Rev. Mod. Phys. **23**, 90 (1951).

[37] I. M. Mills, in *Molecular Spectroscopy: Modern Research*, edited by K. N. Rao and C. W. Mathews (Academic, New York, 1972), pp. 115–140.

[38] D. Papoušek and M. R. Aliev, *Molecular Vibrational-Rotational Spectra* (Elsevier, Amsterdam, 1982).

[39] E. L. Sibert III, J. Chem. Phys. **88**, 4378 (1988).

[40] K. Aarset, A. G. Császár, E. L. Sibert III, W. D. Allen, H. F. Schaefer III, W. Klopper, and J. Noga, J. Chem. Phys. **112**, 4053 (2000).

[41] C. Iung, F. Ribeiro, and E. L. Sibert III, J. Phys. Chem. A **110**, 5420 (2006).

[42] W. H. Miller, N. C. Handy, and J. E. Adams, J. Chem. Phys. **72**, 99 (1980).

[43] S. Carter, J. M. Bowman, and N. C. Handy, Theor. Chem. Acc. **100**, 191 (1998).

[44] S. Carter and J. M. Bowman, J. Chem. Phys. **108**, 4397 (1998).

[45] S. Carter and N. C. Handy, J. Chem. Phys. **113**, 987 (2000).

[46] T. Carrington and W. H. Miller, J. Chem. Phys. **81**, 3942 (1984).

[47] J. M. Bowman, Adv. Chem. Phys. **61**, 115 (1985).

[48] T. Carrington and W. H. Miller, J. Chem. Phys. **84**, 4364 (1986).

[49] G. D. Billing, Mol. Phys. **89**, 355 (1996).

[50] E. Mátyus, G. Czakó, and A. G. Császár, J. Chem. Phys. **130**, 134112 (2009).

[51] B. Fehrensen, D. Luckhaus, and M. Quack, Chem. Phys. Lett. **300**, 312 (1999).

[52] D. Luckhaus, J. Chem. Phys. **113**, 1329 (2000).

[53] D. Luckhaus, J. Chem. Phys. **118**, 8797 (2003).

[54] D. Lauvergnat and A. Nauts, J. Chem. Phys. **116**, 8560 (2002).

[55] S. N. Yurchenko, W. Thiel, and P. Jensen, J. Mol. Spectrosc. **245**, 126 (2007).

[56] A. G. Császár and N. C. Handy, J. Chem. Phys. **102**, 3962 (1995).

[57] M. Quack, J. Stohner, and M. Willeke, Annu. Rev. Phys. Chem. **59**, 741 (2008).

[58] P. R. Bunker, P. Jensen, *Molecular Symmetry and Spectroscopy*, 2nd ed. (NRC Research, Ottawa, 1998).

[59] J. Tennyson, J. Chem. Phys. **98**, 9658 (1993).

[60] T. Furtenbacher, G. Czakó, B. T. Sutcliffe, A. G. Császár, and V. Szalay, J. Mol. Struct. **780**, 283 (2006).

[61] J. Tennyson, J. R. Henderson, and N. G. Fulton, Comput. Phys. Commun. **86**, 175 (1995).

[62] J. Tennyson, M. A. Kostin, P. Barletta, G. J. Harris, O. L. Polyansky, J. Ramanlal, and N. F. Zobov, Comput. Phys. Commun. **163**, 85 (2004).

[63] D. Schwenke, J. Phys. Chem. **100**, 2867 (1996).

[64] I. N. Kozin, M. M. Law, J. Tennyson, and J. M. Hutson, Comput. Phys. Commun. **163**, 117 (2004).

[65] X.-G. Wang and T. Carrington, J. Chem. Phys. **121**, 2937 (2004).

[66] H. G. Yu, J. Chem. Phys. **117**, 8190 (2002).

[67] X. Huang, D. W. Schwenke, and T. J. Lee, J. Chem. Phys. **129**, 214304 (2008).

[68] S. N. Yurchenko, M. Carvajal, P. Jensen, H. Lin, J. Zheng, and W. Thiel, Mol. Phys. **103**, 359 (2005).

[69] S. N. Yurchenko, R. J. Barber, A. Yachmenev, W. Thiel, P. Jensen, and J. Tennyson, J. Phys. Chem. A **113**, 11845 (2009).

[70] H. Goldstein, *Classical Mechanics* (Addison-Wesley, Reading, MA, 1980).

[71] R. N. Zare, *Angular Momentum: Understanding Spatial Aspects in Chemistry and Physics* (Wiley-Interscience, New York, 1988).

[72] G. O. Sørensen, Top. Curr. Chem. **82**, 99 (1979).

[73] See supplementary material at http://dx.doi.org/10.1063/1.3533950 for the derivation of Eqs. (10), (12), and (13) and for a pictorial representation of the deviations between the convergent and approximate rovibrational levels (Figure S1).

[74] E. B. Wilson, J. C. Decius, and P. C. Cross, *Molecular Vibrations* (McGraw-Hill, New York, 1955).

[75] B. Podolsky, Phys. Rev. **32**, 812 (1928).

[76] L. Halonen, in *Computational Molecular Spectroscopy*, edited by P. Jensen and P. R. Bunker (Wiley, Chichester, 2000), pp. 325–364.

[77] B. Schutz, *Geometrical Methods in Mathematical Physics* (Cambridge University Press, Cambridge, 1980).

[78] J. K. G. Watson, J. Mol. Spectrosc. **228**, 645 (2004).

[79] T. J. Lukka, J. Chem. Phys. **102**, 3945 (1995).

[80] S. M. Colwell and N. C. Handy, Mol. Phys. **92**, 317 (1997).

[81] C. Lanczos, J. Res. Natl. Bur. Stand. **45**, 255 (1950).

[82] S. N. Yurchenko, J. Zheng, H. Lin, P. Jensen, and W. Thiel, J. Chem. Phys. **123**, 134308 (2005).

[83] J. Echave and D. C. Clary, Chem. Phys. Lett. **190**, 225 (1992).

[84] H. Wei and T. Carrington, Jr, J. Chem. Phys. **97**, 3029 (1992).

[85] V. Szalay, G. Czakó, Á. Nagy, T. Furtenbacher, and A. G. Császár, J. Chem. Phys. **119**, 10512 (2003).

[86] H. C. Longuet-Higgins, Mol. Phys. **6**, 445 (1963).

[87] A. G. Császár, W. D. Allen, and H. F. Schaefer, J. Chem. Phys. **108**, 9751 (1998).

[88] W. Klopper, C. C. M. Samson, G. Tarczay, and A. G. Császár, J. Comput. Chem. **22**, 1306 (2001).

[89] E. Mátyus, C. Fábri, T. Szidarovszky, G. Czakó, W. D. Allen, and A. G. Császár, J. Chem. Phys. **133**, 034113 (2010).

[90] T. Rajamäki, A. Miani, and L. Halonen, J. Chem. Phys. **118**, 6358 (2003).

[91] S. N. Yurchenko, personal communication (August 18, 2010).

[92] O. L. Polyansky, A. G. Császár, S. V. Shirin, N. F. Zobov, P. Barletta, J. Tennyson, D. W. Schwenke, and P. J. Knowles, Science **299**, 539 (2003).

[93] A. G. Császár, G. Czakó, T. Furtenbacher, J. Tennyson, V. Szalay, S. V. Shirin, N. F. Zobov, and O. L. Polyansky, J. Chem. Phys. **122**, 214305 (2005).

[94] S. V. Shirin, O. L. Polyansky, N. F. Zobov, R. I. Ovsyannikov, A. G. Császár, and J. Tennyson, J. Mol. Spectrosc. **236**, 216 (2006).

[95] M. Artamonov, T.-S. Ho, and H. Rabitz, Chem. Phys. **328**, 147 (2006).